J. Fluid Mech. (1977), *vol.* 79, *part* 1, *pp.* 71–92
Printed in Great Britain

Harbour resonance due to set-down beneath wave groups

By E. C. BOWERS
Hydraulics Research Station, Wallingford, Oxfordshire OX10 8BA

(Received 5 December 1975)

Natural modes of water oscillation inside harbours are known to occur with periods of the order of minutes. It seems likely that these oscillations are excited by water fluctuations of similar period outside the harbour and an often quoted cause of such fluctuations is the phenomenon of surf beats. These are thought to be long waves which are reflected back out to sea when a primary wave system breaks upon a beach. In this paper it is shown theoretically that the natural oscillations of a harbour can be excited directly, without breaking of the primary wave system, by set-down beneath wave groups, which is a long-period disturbance travelling towards the shore line at the group velocity. This theory is in agreement with model experimental results which show that, when the group period is close to a natural period of the harbour, resonance will occur with the set-down behaving as if it were a real long wave.

1. Introduction

The frequency spectra of sea waves are typically narrow band. In particular, a group period, which is just the reciprocal of the difference between typical wave frequencies, will be longer than wave periods. Thus waves tend to travel in well-defined groups in the sea.

One effect of wave grouping is to cause set-down beneath wave groups, which is a phenomenon that was first described by Longuet-Higgins & Stewart (1964). The mechanism producing set-down can be explained in the following way. The velocity of water particles due to wave motion will clearly be large in groups of high waves compared with the water velocity in between the groups. As indicated by Bernoulli's equation this will tend to cause a reduction in water pressure which is proportional to the square of the water particle velocity. Thus the water pressure will tend to be low beneath groups of high waves compared with the pressure in between the groups. If the usual assumption of constant air pressure is made then the mean water level will become depressed beneath the groups and a corresponding rise in the mean level will occur between the groups. This surface perturbation will tend to induce a wavelike flow beneath the surface and so a long-period disturbance is formed. In deep water, surface waves move through the groups with twice the group velocity and so the group pattern is continually changing. This prevents the set-down from building up. However, when the primary wave system moves into shallow water, where waves travel only slightly faster than the group, a more persistent group pattern will occur which allows a larger set-down to form. Using the formula derived by Longuet-Higgins & Stewart (1964), the set-down is shallow water ($kd \ll 1$) beneath groups of waves of amplitude a is given by

$$\bar{\zeta} = -3ga^2/2\omega^2 d^2.$$

Thus, for swell waves of period 15 s and amplitude 1 m this formula gives an associated set-down in a depth of 20 m of order 0·2 m. Therefore, apart from the obvious rapid increase in set-down with wave height, which will lead to significant long-period disturbances as storm waves reach the coastline, quite large set-downs will also be associated with swell waves of moderate height.

Tucker (1950) reported a correlation, which occurred off a beach in Cornwall, between fluctuations of period of the order of minutes and the envelope of incoming waves. This correlation occurred with the long waves lagging behind the wave envelope by 4–5 min. It was suggested by Longuet-Higgins & Stewart (1964) that the time lag in these long waves or surf beats corresponded to the time taken for the ordinary waves to propagate into the breaker zone and for the associated long-period fluctuations to be reflected back as a free wave. Thus surf beats are thought to be long waves which propagate out to sea after being generated by ordinary waves breaking on a beach. Wilson (1957) has discussed the possibility that surf beats as well as barometric pressure variations could be responsible for exciting harbour resonances of period of the order of minutes.

The mechanism whereby set-up occurs on a beach shorewards of the breaker zone was also described by Longuet-Higgins & Stewart (1964). Set-up has been observed by Saville (1961) and consists of a gradual rise in the mean water level as a breaking wave travels up a beach. Bowen & Inman (1971) have shown how set-up shorewards of a breaking zone can become coupled with waves propagating parallel to a beach and form a standing edge-wave pattern when the beach is bounded by prominent headlands. Clarke (1974) has suggested that such edge waves formed on a beach near Port Kembla could be responsible for the excitation of resonant modes of the harbour.

The above arguments indicate that surf beats and edge waves are generated by ordinary waves breaking on a beach. Thus two of the frequently quoted causes of harbour resonance rely on the presence of a beach near the harbour. In this paper theoretical and model experimental results are presented which show that the natural modes of water oscillation of a harbour can be excited by set-down beneath wave groups. This mechanism of harbour resonance differs from excitation due to surf beats or edge waves in that it is no longer necessary to have ordinary waves breaking on a beach near the harbour.

To the author's knowledge no one has previously demonstrated that set-down, which is not a true long wave because it propagates at the group velocity, can excite long waves inside harbours. However, the theoretical work presented in this paper shows that when a Stokes expansion of the wave equations is carried out to second order in the wave amplitude an imbalance occurs between the long-period fluctuations in the water pressure inside and outside the harbour entrance. This imbalance arises because primary wave heights inside the harbour are different from wave heights outside, giving rise to different set-downs inside and outside

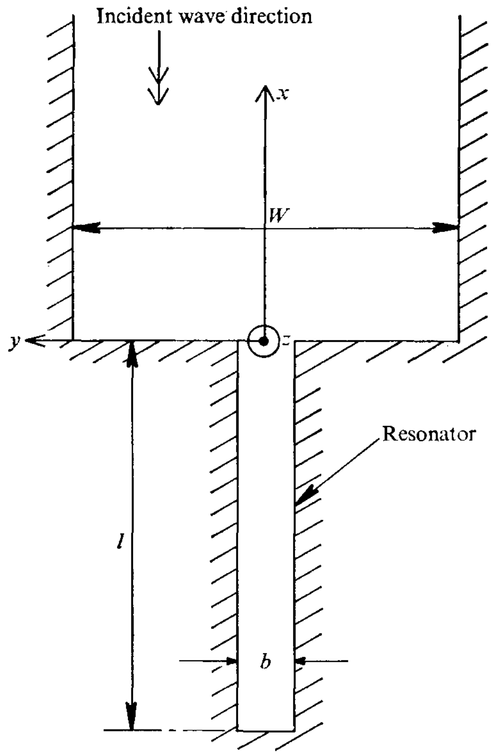

FIGURE 1. Plan view of the set-up assumed for the theoretical calculations.

the harbour. Thus, in order to match water pressures across the harbour entrance it is necessary to introduce an additional velocity potential which obeys the usual wave conditions. In other words, it becomes necessary to introduce a real long wave for purposes of continuity and it is this long wave that will be amplified when the group period is close to a natural period of the harbour.

In §2 a calculation is made of the response of a geometrically simple harbour to water waves. In §3 the calculation is taken to second order in the Stokes expansion of the wave equations for the case of a primary wave system made up of two frequencies. The form of the additional velocity potential required for continuity of pressure is obtained and its significance for a real harbour is discussed. Section 4 contains experimental results obtained by using a model harbour which was subjected to a primary wave system consisting of two frequencies. Evidence is presented for the existence in the experiments of a secondary wave with a frequency of oscillation equal to the group frequency of the primary wave system. However, it is shown that the model harbour responded to the resultant of the secondary wave, which is purely a model effect, and the set-down, which can be expected in a real sea. This leads to the final conclusion that a real harbour will respond to set-down beneath wave groups in the manner indicated by the theoretical work. Finally, an appendix contains a derivation of the velocity potential of the secondary wave.

2. First-order harbour response

Here the response of a geometrically simple resonator to water waves is calculated. The resonator consists of a long narrow channel blocked off at one end and open at the other which is joined to a wave flume wider than the channel. A wave flume is assumed to exist outside the resonator simply in order to make calculation of second-order potentials more manageable. The configuration, which is shown in figure 1, can be expected to retain some of the features of a harbour basin open to the sea. Incident and reflected waves are assumed to travel parallel to the wave flume and resonating channel, in the x direction, where x, y and z form the right-handed orthogonal co-ordinate system shown in figure 1, with the still water level occurring at $z = 0$. The basic equation for incompressible irrotational motion is

$$\nabla^2\phi = 0, \tag{1}$$

where the fluid velocity is

$$\mathbf{q} = (u, v, w) = -\nabla\phi.$$

The boundary conditions are

$$w = 0 \tag{2}$$

on the bottom $z = -d$ and

$$\eta_t + u\eta_x + v\eta_y - w = 0, \tag{3}$$

$$\tfrac{1}{2}q^2 + g\eta - \phi_t = 0, \tag{4}$$

on the free surface $z = \eta$.

If a wave of amplitude a is incident on the resonator the appropriate form for the first-order velocity potential outside the resonator is

$$\phi^{(1)} = \frac{ig\cosh k(z+d)}{\omega\cosh kd}\,[a(e^{-ikx}+e^{ikx})+f(x,y)]\,e^{-i\omega t}. \tag{5}$$

Here the first term represents the incident wave, the second its reflexion from the wall at $x = 0$ and the third term is the wave radiated from the mouth of the resonator. Equation (1) and the boundary conditions (2)–(4) are satisfied to first order by the potential given in (5) provided that

$$f_{xx} + f_{yy} + k^2 f = 0 \tag{6}$$

and the dispersion relation for surface waves is satisfied, i.e.

$$\omega^2 = kg\tanh kd. \tag{7}$$

The solution for f which satisfies $v = 0$ on $y = \pm\frac{1}{2}W$ (the walls of the wave flume) can be written in the form

$$f = \sum_{N=0}^{\infty} A_N \cos\frac{N\pi}{W}\left(y+\frac{W}{2}\right)\exp(-\beta_n x),$$

where (6) gives

$$\beta_N = [(N\pi/W)^2 - k^2]^{\frac{1}{2}}.$$

Let the wave slope at the harbour entrance be represented by $C\,e^{-i\omega t}$. Then at $x = 0$

$$-\sum_{N=0}^{\infty} \beta_N A_N \cos\frac{N\pi}{W}\left(y+\frac{W}{2}\right) = \begin{cases} C \text{ for } |y| \leqslant \frac{1}{2}b, \\ O \text{ for } \frac{1}{2}b \leqslant |y| \leqslant \frac{1}{2}W. \end{cases}$$

Multiplying both sides of the above equation by $\cos N\pi W^{-1}(y+\frac{1}{2}W)$ and integrating over the range $|y| \leqslant \frac{1}{2}W$ gives

$$A_0 = \frac{-ibC}{kW}, \quad A_{2N} = \frac{(-1)^{N+1}2C\sin(N\pi b/W)}{N\pi\beta_{2N}}, \quad A_{2N+1} = 0.$$

For simplicity the wavelength $2\pi/k$ is assumed to be larger than the flume width W so that the dominant term in the radiated wave will be independent of y. Then the first-order potential outside the resonator becomes

$$\phi^{(1)} = \frac{ig\cosh k(z+d)}{\omega\cosh kd}\left[a(e^{-ikx}+e^{+ikx}) - \frac{ibC}{kW}e^{ikx}\right]e^{-i\omega t}.$$

The first-order potential inside the resonator, which satisfies $u = 0$ on $x = -l$ (the end of the resonator), will take the form

$$\phi^{(1)} = \frac{iDg\cosh k(z+d)}{\omega\cosh kd}\{\exp[ik(x+l)] + \exp[-ik(x+l)]\}e^{-i\omega t}.$$

The boundary condition on wave slope at $x = 0$ requires

$$-2kD\sin kl = C.$$

Continuity of potential across the harbour entrance (of width b) requires

$$2D\cos kl = 2a - ibC/kW.$$

Solving these two simultaneous equations for D and C gives

$$C = \frac{-2ka\sin kl}{\cos kl - ibW^{-1}\sin kl}, \quad D = \frac{a}{\cos kl - ibW^{-1}\sin kl}.$$

Thus the largest response inside the harbour is obtained when

$$kl = \tfrac{1}{2}(2n+1)\pi, \quad n = 0, 1, 2, \ldots, \tag{8}$$

i.e.
$$\lambda = 2\pi/k = 4l/(2n+1),$$

and the amplification factor, which is defined to be the wave height at $x = -l$ divided by $2a$, is W/b. In particular, the longest resonant wave ($n = 0$) has a wavelength equal to four times the length of the resonator.

Summarizing, one can say that for waves incident on the resonator the velocity potential outside takes the form

$$\phi^{(1)} = \frac{g\cosh k(z+d)}{\omega\cosh kd}[a\sin(\omega t+kx) + a\sin(\omega t-kx) - e\cos(\omega t-kx-\alpha)] \tag{9}$$

while the potential inside has the form

$$\phi^{(1)} = \frac{g|D|\cosh k(z+d)}{\omega\cosh kd}\{\sin[\omega t+k(x+l)-\alpha] + \sin[\omega t-k(x+l)-\alpha]\}, \tag{10}$$

where
$$e = b|C|/Wk, \quad |D| = a/(\cos^2 kl + b^2W^{-2}\sin^2 kl)^{\frac{1}{2}}, \tag{11}$$

$$|C| = 2k|D|\sin kl, \quad \tan\alpha = bW^{-1}\tan kl.$$

The response of the resonator is taken to second order in the next section, where use is made of the first-order potentials (9) and (10).

3. Second-order harbour response

Here the second-order potentials describing flow induced by set-down beneath wave groups are derived, both inside and outside the resonator. These potentials will then be matched across the entrance to the resonator.

When the second-order wave elevation given by (4) is substituted into (3) and use is made of the approximations

$$(\phi_t^{(2)})_{z=\eta} \cong \phi_t^{(2)}(z=0)+\eta^{(1)}\phi_{tz}^{(1)}(z=0),$$

$$(w^{(2)})_{z=\eta} \cong w^{(2)}(z=0)+\eta^{(1)}w_z^{(1)}(z=0),$$

one obtains the boundary condition to be satisfied at $z=0$ in the form

$$\phi_{tt}^{(2)}+g\phi_z^{(2)} = \eta^{(1)}(w_{tt}^{(1)}+gw_z^{(1)})+2\mathbf{q}^{(1)}\cdot\mathbf{q}_t^{(1)}. \tag{12}$$

This equation can be interpreted as a surface perturbation on the right-hand side inducing the second-order potential flow on the left-hand side.

If it is assumed that two sine waves are incident on the resonator, then, using (9), the first-order potential outside the resonator will take the form

$$\phi_{\text{out}}^{(1)} = \sum_{j=1,2}\frac{g\cosh k_j(z+d)}{\omega_j\cosh k_j d}[a_j\sin(\omega_j t+k_j x)+a_j\sin(\omega_j t-k_j x) \\ -e_j\cos(\omega_j t-k_j x-\alpha_j)].$$

This potential may be used to evaluate the terms appearing on the right-hand side of (12). These terms consist of products of first-order quantities and their fluctuating parts may be expressed as sines and cosines with arguments of the form

$$\omega^- t\pm k^- x,\quad \omega^- t\pm k^+ x,\quad \omega^+ t\pm k^+ x,\quad \omega^+ t\pm k^- x,$$

$$2(\omega_j t\pm k_j x),\quad j=1,2,$$

where

$$\omega^\pm = \omega_2\pm\omega_1,\quad k^\pm = k_2\pm k_1.$$

Since the main interest in this paper is the excitation of harbour resonances of period of the order of minutes and the sum frequency ω^+ can be expected to give fluctuations on the scale of seconds, only those terms involving the difference frequency ω^- will be retained. Let the part of the second-order potential fluctuating at the difference frequency be denoted by $\tilde{\phi}^{(2)}$. This potential must satisfy (1) and (2) as well as the surface condition (12) and is found to take the form

$$\tilde{\phi}_{\text{out}}^{(2)} = A\cosh k^-(z+d)\{a_1a_2[\sin(\omega^- t+k^- x)+\sin(\omega^- t-k^- x)] \\ -a_1e_2\cos(\omega^- t-k^- x-\alpha_2)+a_2e_1\cos(\omega^- t-k^- x+\alpha_1) \\ +e_1e_2\sin(\omega^- t-k^- x-\alpha^-)\}+B\cosh k^+(z+d)\{a_1a_2[\sin(\omega^- t+k^+ x) \\ +\sin(\omega^- t-k^+ x)]-a_1e_2\cos(\omega^- t-k^+ x-\alpha_2)+a_2e_1\cos(\omega^- t+k^+ x+\alpha_1)\}, \tag{13}$$

where A and B are defined by

$$A\{(\omega^-)^2\cosh k^-d - gk^-\sinh k^-d\} = \frac{\omega^- k_1 k_2 g^2}{\omega_1\omega_2}(1+\tanh k_1 d\tanh k_2 d) + \frac{gk_1}{2\omega_1}(\omega_1^2\tanh k_1 d - gk_1) - \frac{gk_2}{2\omega_2}(\omega_2^2\tanh k_2 d - gk_2), \tag{14}$$

$$B\{(\omega^-)^2\cosh k^+d - gk^+\sinh k^+d\} = \frac{\omega^- k_1 k_2 g^2}{\omega_1\omega_2}(1-\tanh k_1 d\tanh k_2 d) + \frac{gk_1}{2\omega_1}(\omega_1^2\tanh k_1 d - gk_1) - \frac{gk_2}{2\omega_2}(\omega_2^2\tanh k_2 d - gk_2). \tag{15}$$

Using (10), the first-order potential representing the response of the resonator to two incident waves will take the form

$$\phi_{\text{in}}^{(1)} = \sum_{j=1,2} \frac{g\cosh k_j(z+d)\,|D_j|}{\omega_j\cosh k_j d}\{\sin[\omega_j t + k_j(x+l) - \alpha_j] + \sin[\omega_j t - k_j(x+l) - \alpha_j]\}.$$

Using this potential to evaluate the right-hand side of the surface condition (12) will lead to the slowly varying part of the second-order potential inside the resonator. This potential must also satisfy (1) and (2) and is found to be

$$\begin{aligned}\tilde{\phi}_{\text{in}}^{(2)} = {} & A\cosh k^-(z+d)|D_1|\,|D_2|\{\sin[\omega^- t + k^-(x+l) - \alpha^-] \\ & + \sin[\omega^- t - k^-(x+l) - \alpha^-]\} \\ & + B\cosh k^+(z+d)\,|D_1|\,|D_2|\{\sin\{\omega^- t + k^+(x+l) - \alpha^-\} \\ & + \sin[\omega^- t - k^+(x+l) - \alpha^-]\},\end{aligned} \tag{16}$$

where A and B are given by (14) and (15) and $\alpha^- = \alpha_2 - \alpha_1$. It can be seen straight away that the boundary condition $u = 0$ at $x = -l$ is automatically satisfied by this expression for $\tilde{\phi}_{\text{in}}^{(2)}$.

In shallow water ($k_j d \ll 1$, $j = 1, 2$) the coefficients A and B reduce to the simple forms

$$A \cong -\frac{3}{2}\left(\frac{g}{d}\right)^{\frac{1}{2}} \frac{4}{k^-d(k^+d)^2}, \quad B \cong -\frac{3}{2}\left(\frac{g}{d}\right)^{\frac{1}{2}}\left(\frac{k^-}{k^+}\right)^2 \frac{1}{k^-d}.$$

Thus $B \cong \frac{1}{4}(k^-d)^2 A$, so that $B \ll A$. It can also be shown that this inequality between A and B holds in deep water ($k_j d \gg 1$) and so from now on those terms involving B in the second-order potential will be neglected both inside and outside the resonator.

Imagining for the moment that the mouth of the resonator is blocked off, one finds that the amplitude of the set-down at the wall $x = 0$ is given approximately by

$$\bar{\zeta} = |\eta^{(2)}| \cong \left|\frac{\tilde{\phi}_t^{(2)}}{g}\right|_{\text{out}} = \frac{2\omega^- A a_1 a_2}{g} \cong -\frac{3ga_1a_2}{\omega^2 d^2}.$$

Comparing this expression with that given in the introduction it can be seen that the set-down associated with a standing wave pattern is twice that associated with progressive waves. The term set-down should only be used to refer to the depression in mean water level which occurs when a group of high waves reflects from the wall. When the waves that make up the primary wave system are out of phase, so that little or no resultant wave will be visible at the wall, then the mean water level is raised, which strictly speaking should be called a set-up, although the latter term is normally used for the phenomenon that occurs when waves break upon a beach.

The boundary conditions to be satisfied at the entrance to the resonator are continuity of the second-order potential and continuity of its derivative with respect to x. Using (16) and remembering that terms involving the coefficient B are being ignored, the derivative just inside the resonator takes the form

$$-2Abk^{-}W^{-1}\cosh k^{-}(z+d)\,|D_1|\,|D_2|\,\sin k^{-}l\sin(\omega^{-}t-\alpha^{-})$$
$$= C^{(2)}\cosh k^{-}(z+d)\sin(\omega^{-}t-\alpha^{-}),\ \text{say}. \quad (17)$$

Thus the condition on the derivative of the second-order potential just outside the resonator is

$$\phi_x^{(2)} = \begin{cases} C^{(2)}\cosh k^{-}(Z+d)\sin(\omega^{-}t-\alpha^{-}) & \text{for} \quad |y| \leqslant \tfrac{1}{2}b, \\ 0 \quad \text{for} \quad \tfrac{1}{2}b < |y| \leqslant \tfrac{1}{2}W. \end{cases}$$

If all the terms in the expression for the radiated primary wave system had been retained then the left-hand side of the above equation would have taken the form of a sum of cosines of linear functions of y. The condition to be satisfied by each coefficient would have been found by multiplying each side of the equation by the appropriate cosine and integrating over the range $|y| \leqslant \frac{1}{2}W$. As only that part of the radiated wave system which is independent of y is of importance for the case being considered in this paper, the above condition on $\bar{\phi}_x^{(2)}$ at $x = 0$ takes the simple form

$$W\bar{\phi}_x^{(2)} = bC^{(2)}\cosh k^{-}(z+d)\sin(\omega^{-}t-\alpha^{-}). \quad (18)$$

Using (13) to evaluate the derivative of $\bar{\phi}^{(2)}$ gives

$$\bar{\phi}_x^{(2)} = Ak^{-}\cosh k^{-}(z+d)\,[(-a_1e_2\cos\alpha_2 + a_2e_1\cos\alpha_1 - e_1e_2\sin\alpha^{-})\sin\omega^{-}t$$
$$+(a_1e_2\sin\alpha_2 + a_2e_1\sin\alpha_1 - e_1e_2\cos\alpha^{-})\cos\omega^{-}t].$$

One can show that this expression for $\bar{\phi}_x^{(2)}$ satisfies (18) after some algebra and use of the definitions given in (11) together with the definition of $C^{(2)}$ given in (17). Thus the boundary condition on the derivatives of the second-order potentials at $x = 0$ is identically satisfied by the potentials given in (13) and (16).

The remaining boundary condition is continuity of the second-order potential itself, in other words second-order pressure, at the entrance to the resonator. Using (16), the potential just inside the resonator is

$$\bar{\phi}^{(2)} = 2A\cosh k^{-}(z+d)\,|D_1|\,|D_2|\cos k^{-}l\sin(\omega^{-}t-\alpha^{-}). \quad (19)$$

The potential just outside the resonator is obtained from (13) and takes the form

$$\bar{\phi}^{(2)} = A \cosh k^-(z+d)\,[(2a_1 a_2 - a_1 e_2 \sin\alpha_2 - a_2 e_1 \sin\alpha_1 + e_1 e_2 \cos\alpha^-) \times \sin\omega^- t + (-a_1 e_2 \cos\alpha_2 + a_2 e_1 \cos\alpha_1 - e_1 e_2 \sin\alpha^-)\cos\omega^- t]. \quad (20)$$

Subtracting the potential given in (20) from that given in (19) gives

$$E \cosh k^-(z+d)\sin(\omega^- t - \alpha^-), \quad (21)$$

where

$$E = \frac{2Aa_1 a_2 (1 - b^2 W^{-2})\sin k_1 l \sin k_2 l}{(\cos^2 k_1 l + b^2 W^{-2}\sin^2 k_1 l)^{\frac{1}{2}}(\cos^2 k_2 l + b^2 W^{-2}\sin^2 k_2 l)^{\frac{1}{2}}}.$$

Thus the second-order potentials do not match across the entrance to the resonator. As mentioned in the introduction, this occurs because different wave heights inside and outside the resonator lead to different amounts of set-down on either side of the entrance. The difficulty is overcome by introducing a second-order potential $\phi_L^{(2)}$ which fluctuates at the difference frequency ω^- and satisfies Laplace's equation together with the boundary conditions

$$w^{(2)} = 0 \quad \text{on} \quad z = -d$$

and

$$\eta_t^{(2)} - w^{(2)} = g\eta^{(2)} - \phi_{Lt}^{(2)} = 0 \quad \text{on the free surface} \quad z = 0.$$

Thus inside the resonator

$$\phi_L^{(2)} = D^{(2)}\cosh K^-(z+d)\,[\sin(\omega^- t + K^-(x+l) - \gamma) + \sin(\omega^- t - K^-(x+l) - \gamma)], \quad (22)$$

while outside the potential representing the radiated wave takes the form

$$\phi_L^{(2)} = e^{(2)}\cosh K^-(z+d)\cos(\omega^- t - K^- x - \gamma), \quad (23)$$

where the wavenumber K^- is defined by

$$(\omega^-)^2 = K^- g \tanh K^- d.$$

More exactly, the radiated potential consists of a sum of terms involving cosines of y but since the wavelengths of interest are much larger than the flume width W only that term which is independent of y need be retained. Since the derivative of the second-order potential $\bar{\phi}^{(2)}$ is continuous across $x = 0$ the second-order potential $\phi_L^{(2)}$ must satisfy continuity of its derivative across $x = 0$. This gives

$$e^{(2)} = -2bW^{-1}D^{(2)}\sin K^- l. \quad (24)$$

The remaining boundary condition is continuity of the total second-order potential $\bar{\phi}^{(2)} + \phi_L^{(2)}$ across $x = 0$. In this requirement the mismatch, given in expression (21), between $\bar{\phi}^{(2)}$ on either side of $x = 0$ is the driving term causing a response in the resonator with its associated radiated wave outside. It may be seen straight away that because the driving term is not a real wave its variation with depth is different from that of a real wave with the same frequency. This means that the response produced should consist of the long wave, represented by (22) and (23), together with a solution localized at the resonator entrance much in the same way as a wave paddle produces a local solution as well as surface waves. Since only long waves are of interest here the local solution will be small and one is justified in assuming

$$\cosh k^-(z+d) \simeq \cosh K^-(z+d).$$

With this assumption, continuity of total potential gives

$$2D^{(2)}\cos K^-l\cos\gamma = e^{(2)}\sin\gamma - E\cos\alpha^-,$$
$$2D^{(2)}\cos K^-l\sin\gamma = e^{(2)}\cos\gamma + E\sin\alpha^-.$$

Substituting for $e^{(2)}$ from (24) gives

$$D^{(2)} = \frac{E}{2(\cos^2 K^-l + b^2 W^{-2}\sin^2 K^-l)^{\frac{1}{2}}},$$

$$\tan\gamma = \frac{\cos K^-l\sin\alpha^- + bW^{-1}\sin K^-l\cos\alpha^-}{\cos K^-l\cos\alpha^- - bW^{-1}\sin K^-l\sin\alpha^-}.$$

It can be seen immediately from the above relation for $D^{(2)}$ that the mismatch E which occurs in $\bar{\phi}^{(2)}$ at the entrance will be amplified inside the resonator by a factor of W/b when the group period corresponds to a natural period of the resonator, i.e.

$$K^-l = \tfrac{1}{2}(2n+1)\pi, \quad n = 0, 1, 2. \tag{25}$$

This mismatch can be interpreted in the following way. In the case of a real harbour of moderate size the primary wave system is unlikely to be amplified owing to dissipation. For the simple resonator being considered here this condition means

$$\cos k_j l \neq 0, \quad j = 1, 2,$$

which, when combined with the inequality $b/W \ll 1$, reduces the mismatch given in (21) to

$$E \simeq 2Aa_1 a_2 \tan k_1 l \tan k_2 l.$$

This can be rewritten in the form

$$E \simeq 2Aa_1 a_2 \frac{\cos k^-l}{\cos k_1 l\cos k_2 l} - 2Aa_1 a_2.$$

In shallow water ($k_j d \ll 1$) one can expect k^- and K^- to be almost equal to one another, leading to

$$\cos k^-l \simeq 0$$

when the resonance condition (25) is satisfied. This reduces E to the magnitude of the set-down potential associated with the standing wave pattern formed outside the resonator entrance, i.e.

$$E \simeq -2Aa_1 a_2.$$

Thus, for a real harbour subject to a primary wave system which satisfies the shallow-water condition ($kd \ll 1$) one can expect amplification of the set-down beneath wave groups when the group period is close to a natural period of the harbour. Further, the amplification takes place as if the set-down just outside the harbour entrance, with amplitude $\bar{\zeta}$ say, were a real long wave of amplitude $\bar{\zeta}$.

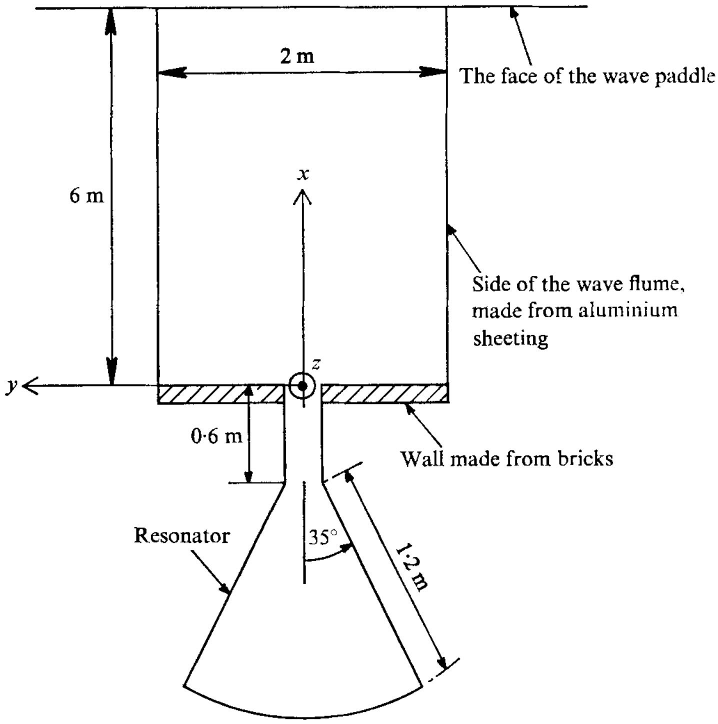

FIGURE 2. Plan view of the model experimental set-up.

4. Comparison between theoretical and experimental results

Experiments were carried out in a wave basin equipped with a piston-driven wave paddle. A plan of the lay-out is shown in figure 2. The model consisted of a wave flume about 2 m wide and 6 m long with sides made from aluminium sheeting. This flume was bounded at one end by the face of the wave paddle and at the other by a wall with a small gap. This gap formed the entrance to the resonator, which consisted of a narrow channel of length 0·6 m leading to a basin in the shape of a sector of a circle with half-angle 35° and radius 1·2 m. The experimental arrangement was chosen in order to avoid the generation of surf beats or edge waves owing to wave breaking. In particular all sides were vertical and the floor was level. Wave heights were measured with a twin-wire wave probe which was connected to a data logger producing magnetic tape for a computer analysis. The data were analysed using a fast Fourier transform computer program to give the spectrum of the wave system. This method of analysis was necessary since estimates of the long-period fluctuations associated with the primary wave system were required.

Initially, monofrequency tests were performed in order to obtain the resonant periods of the model harbour. The Helmholtz resonance or pumping mode, which consisted of a fairly even rise and fall of the water level in the harbour basin with large horizontal flows in the entrance channel, occurred with period about 20 s. This mode is the counterpart of that found in the last section for a blocked-off

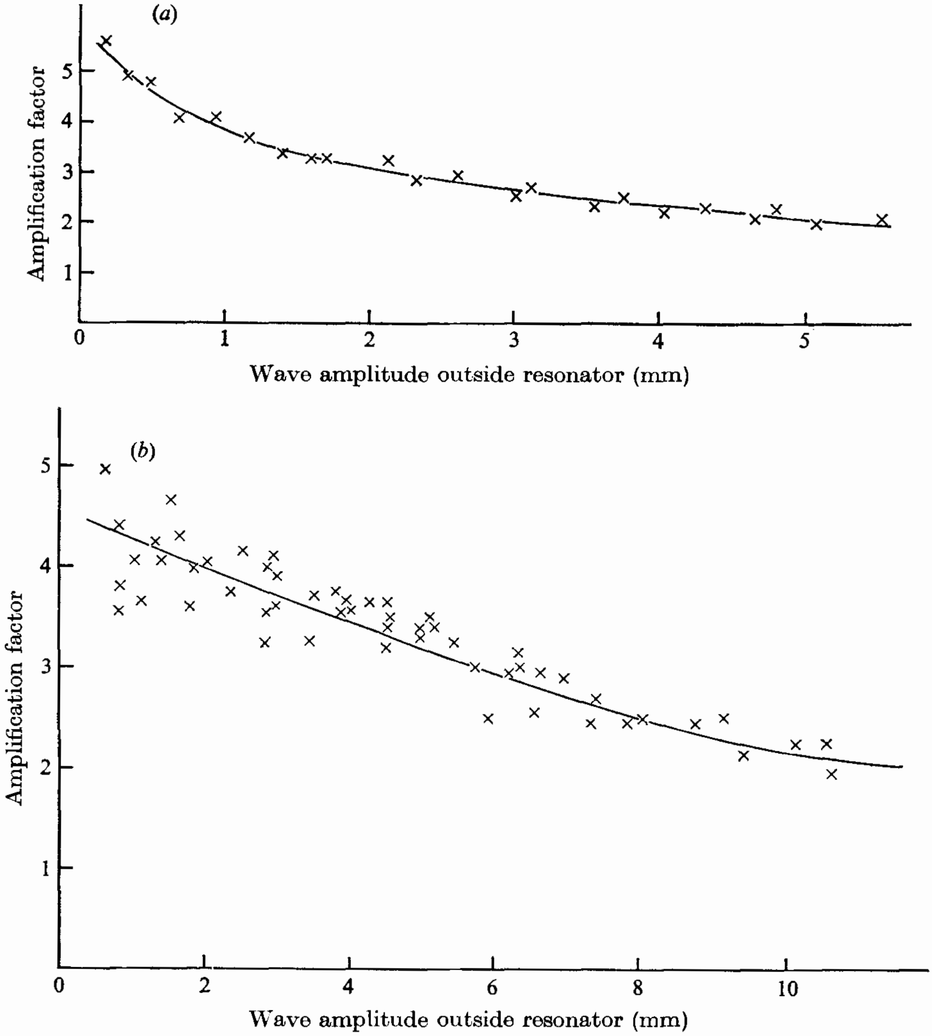

FIGURE 3. A graph showing variation of the amplification factor with external wave height for (*a*) the Helmholtz resonance and (*b*) the sloshing mode.

entrance channel, where the resonant wavelength equals four times the channel length. The sloshing mode occurred with period about 3 s and consisted of an antinode along the curved back wall of the resonator, a nodal line inside the harbour basin and a second antinode in the entrance channel. This type of resonance also occurs in a closed basin, where the resonant wavelength equals twice the basin length.

Separation of horizontal flows at each end of the entrance channel was very noticeable in the experimental work, particularly in the case of the Helmholtz resonance. The effect of separation is shown clearly in figures 3 (*a*) and (*b*). These display the variation of the amplification factor, for the Helmholtz and sloshing modes respectively, as a function of the wave amplitude outside the resonator. The amplification factor is defined as the ratio of the maximum wave height

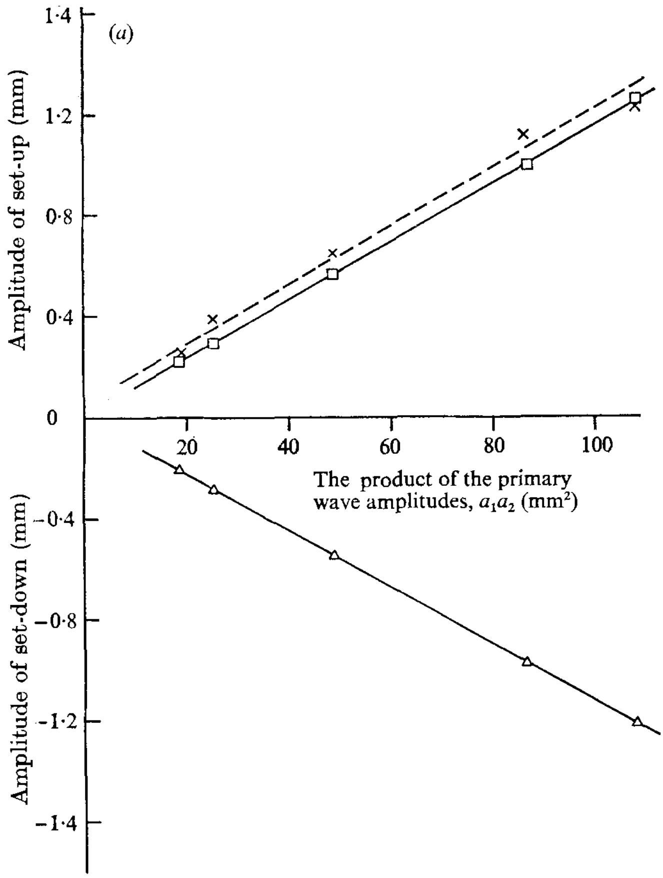

FIGURE 4 (*a*). For caption see p. 85.

occurring in the resonator to the wave height measured in front of the wall outside the resonator. For the Helmholtz resonance the maximum wave height occurred along the back wall of the resonator but for the sloshing mode the wave height was a maximum at the antinode in the entrance channel. All measurements of wave heights outside were carried out with the mouth of the resonator blocked off. Clearly, if the harbour had been obeying linear theory a horizontal line would have been obtained in figures 3 (*a*) and (*b*). The fall-off with increasing wave height obtained in the experiments appears to be consistent with a loss of energy proportional to the square of wave velocity, which is the sort of effect one expects from flow separation. These results imply that for real harbours with narrow entrances the turbulence caused at the harbour mouth is an effective dissipation mechanism for long waves.

Having obtained the model harbour's response at the two longest resonant periods, the next set of experiments was carried out using a wave system made up of two frequencies f_1 and f_2 higher than the resonant frequencies, but with a difference equal to one of the resonant frequencies already mentioned. The purpose of these experiments was to obtain the harbour's response to the long-period fluctuations associated with such a wave system. The total wave system was

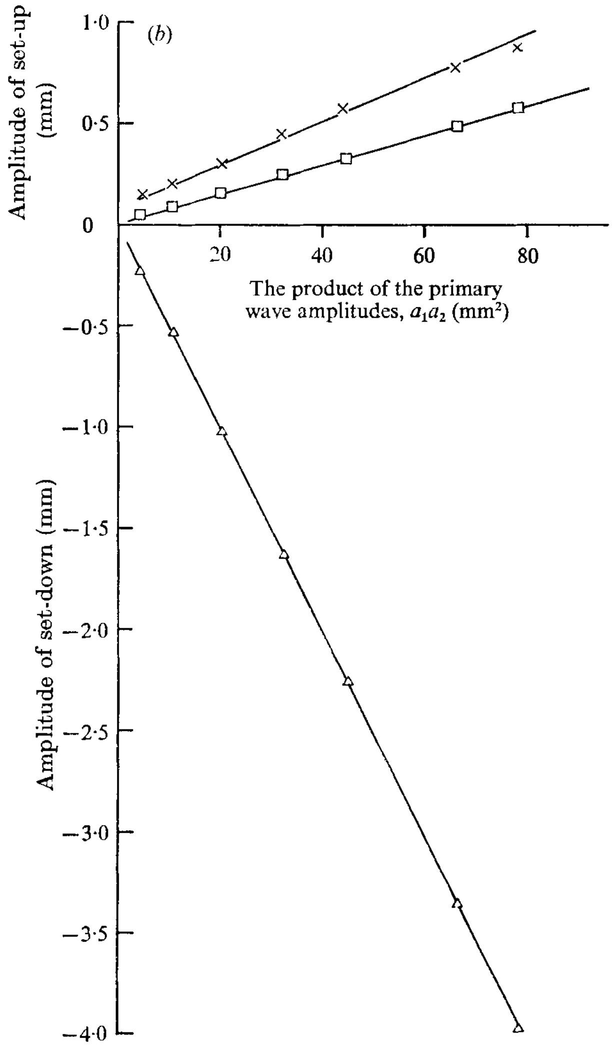

FIGURE 4 (*b*). For caption see p. 85.

measured just in front of the wall outside the resonator with the mouth of the resonator blocked off. The results of these experiments are shown by the crosses in figures 4 (*a*), (*b*) and (*c*) respectively for the following cases: $f_1 = 1{\cdot}0$ Hz with $f_2 - f_1 = 0{\cdot}0475$ Hz (the Helmholtz resonance), $f_1 = 0{\cdot}6$ Hz with $f_2 - f_1 = 0{\cdot}0475$ Hz, $f_1 = 0{\cdot}65$ Hz with $f_2 - f_1 = 0{\cdot}34$ Hz (the sloshing mode). These graphs show the amplitude of the long-period fluctuations as a function of the product of the two primary wave amplitudes. The amplitude of the long-period disturbance was obtained from the following formula for a wave of amplitude a:

$$a_{\text{r.m.s.}} = (\tfrac{1}{2}a^2)^{\frac{1}{2}},$$

where $a_{\text{r.m.s.}}$ is the square root of the area under the low frequency hump in the spectrum measured in front of the wall. A typical such spectrum is shown in

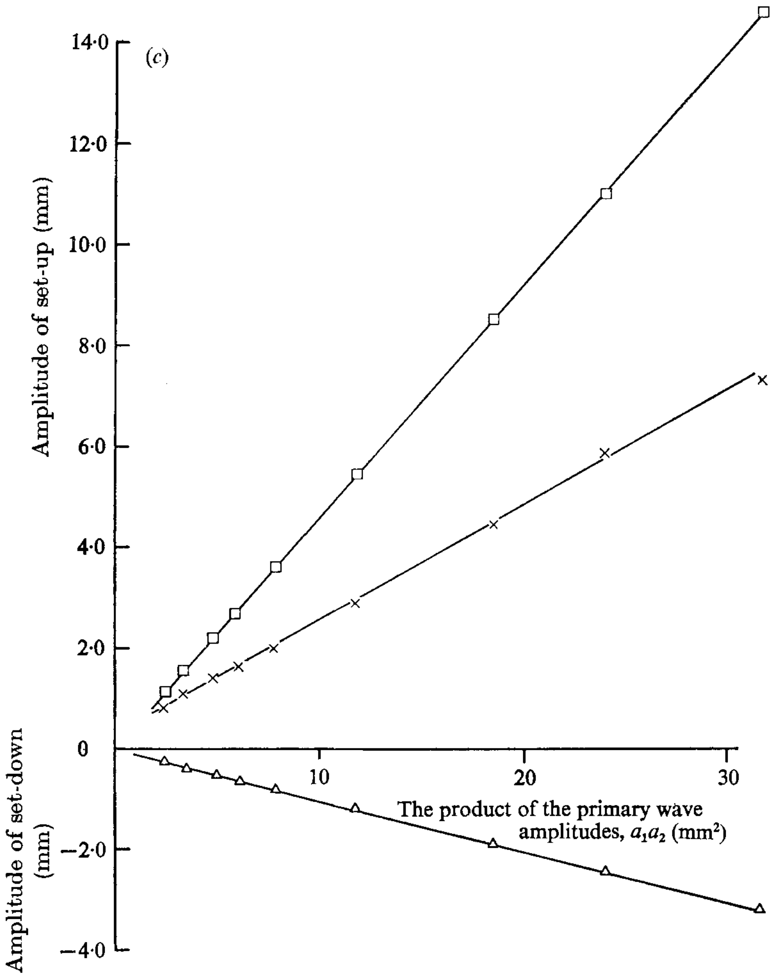

FIGURE 4. Amplitude of the long-period fluctuations versus a_1a_2 for (*a*) $f_1 = 1{\cdot}0$ Hz, $f_2 = 1{\cdot}0475$ Hz, (*b*) $f_1 = 0{\cdot}6$ Hz, $f_2 = 0{\cdot}6475$ Hz and (*c*) $f_1 = 0{\cdot}65$ Hz, $f_2 = 0{\cdot}99$ Hz. – – × – –, experimental values of set-up; — □ —, theoretical values of set-up obtained when secondary wave was included; — △ —, theoretical values of set-down obtained without secondary wave.

figure 5. The two main peaks represent the two waves of the primary system and the areas under these peaks were used to obtain the amplitudes of the primary waves, while the low-frequency hump occurring at the difference frequency is the associated long-period disturbance. Although the primary waves occur at distinct frequencies their spectral lines are broadened owing to smoothing introduced in the analysis.

It was noticed on traces of wave movement that the mean water level appeared to rise beneath a group of large waves and to fall in between the groups. Figure 6 is a trace showing this effect with the mean level indicated by the dotted line. Thus the experiments showed that the long-period fluctuations consisted of a set-up beneath wave groups instead of the expected set-down. This can be

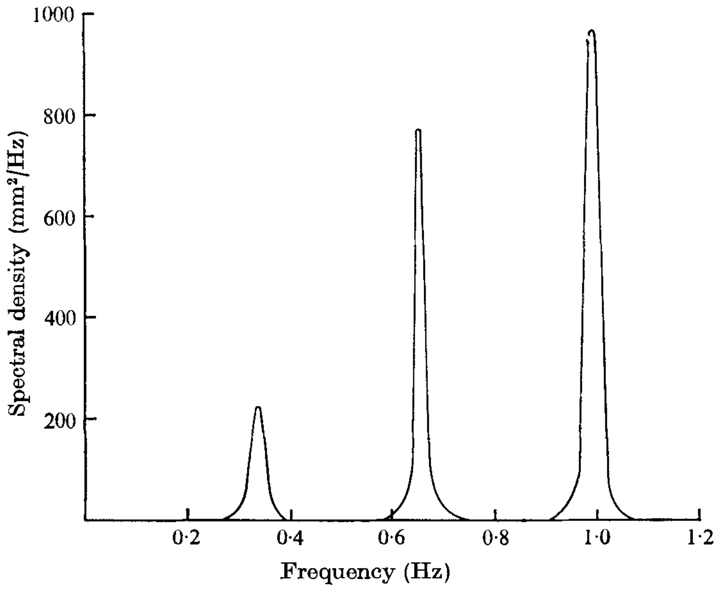

FIGURE 5. A spectral plot showing the primary waves and the long-period fluctuations at the difference frequency.

explained by the presence of a secondary free wave occurring with the same frequency as the set-down. This secondary wave is introduced by the wave paddle and occurs because the second-order expansion performed in the last section indicates that a stable sea with groups of waves present must have the associated set-down tied to the groups but the wave paddle is only programmed to produce the primary waves without the set-down. Thus the boundary condition on the paddle face requires the second-order horizontal water velocity $u^{(2)}$ to vanish. This is achieved by introducing a real long wave with the same frequency as the set-down but with a phase shift of 180° so that the horizontal fluid velocity due to set-down is cancelled on the paddle face by the horizontal velocity due to the free wave. Since the secondary wave is a real wave it propagates away from the paddle slightly faster than the set-down, which travels at the group velocity. Thus the secondary wave is free in the sense that it is not tied to the groups of primary waves. In the experiments described here the secondary waves are very long, so that their phase velocity is only just greater than the group velocity. This means that by the time the set-down and secondary wave have reached the wall at the other end of the wave flume they will still be out of phase. This implies that cancellation of set-down by the secondary wave can be expected at the wall. Indeed, if the secondary wave has a larger amplitude than the set-down, one can expect to observe a set-up in measurements carried out at the wall, which appears to explain the experimental results obtained.

In more detail, the second-order surface elevation in front of the wall is given by (4):

$$\eta^{(2)} = g^{-1}(\phi_t^{(2)} + \eta^{(1)}\phi_{tz}^{(1)} - \tfrac{1}{2}\{\mathbf{q}^{(1)}\}^2), \tag{26}$$

where the left-hand side is evaluated at $x = 0$, $z = 0$. Without the secondary wave, the usual set-down is obtained by using the slowly varying part of $\phi^{(2)}$

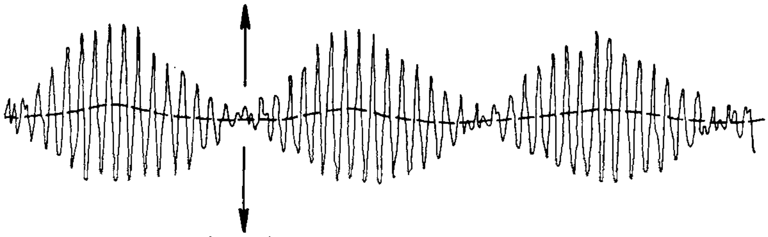

FIGURE 6. A wave trace showing set-up beneath wave groups.

associated with the two primary waves which reflect at $x = 0$. This is given in the first term of (13) (the term with coefficient B has already been shown to be small and so is ignored), i.e.

$$\tilde{\phi}^{(2)} = A a_1 a_2 \cosh k^-(z+d) \left[\sin(\omega^- t + k^- x) + \sin(\omega^- t - k^- x)\right], \tag{27}$$

where A is defined in (14). The first-order potential representing the two primary waves takes the form

$$\phi^{(1)} = \sum_{j=1,2} \frac{a_j g \cosh k_j(z+d)}{\omega_j \cosh k_j d}\left[\sin(\omega_j t + k_j x) + \sin(\omega_j t - k_j x)\right]. \tag{28}$$

Using (27) and (28) to evaluate the slowly varying part of (26) gives the following expression for the set-down at the wall:

$$\begin{aligned}\tilde{\eta}^{(2)} &= a_1 a_2 \left[\frac{2\omega^-}{g} A \cosh k^- d + 2(k_1 \tanh k_1 d + k_2 \tanh k_2 d)\right.\\ &\qquad \left. - \frac{g k_1 k_2 (\cosh k^+ d - \cosh k^- d)}{\omega_1 \omega_2 \cosh k_1 d \cosh k_2 d}\right] \cos \omega^- t \\ &= \bar{\zeta} \cos \omega^- t.\end{aligned} \tag{29}$$

The values of $\bar{\zeta}$ appropriate to the experiments carried out are shown as the theoretical curves joining triangles in figures 4(*a*)–(*c*). As all these values are negative and since $\omega^- t = 2n\pi$ (n integral) when the two primary waves are in phase with one another, (29) clearly implies that set-down should occur beneath large waves.

If the second-order potential due to the secondary wave at the difference frequency is added to the second-order potential representing set-down and the sum used to calculate the $\phi_t^{(2)}$ appearing in (26), a value of $\bar{\zeta}$ more appropriate to the model experiments should be obtained. This is achieved by using equation (A 4) (see appendix) as well as (27) and (28) to evaluate the slowly varying part of the right-hand side of (26). In this way the following equation is obtained:

$$\begin{aligned}\tilde{\eta}^{(2)} &= a_1 a_2 \left\{2\omega^- g^{-1}(A \cosh k^- d + X \cosh K^- d) + 2(k_1 \tanh k_1 d + k_2 \tanh k_2 d)\right.\\ &\quad \left. - \frac{g k_1 k_2 (\cosh k^+ d - \cosh k^- d)}{\omega_1 \omega_2 \cosh k_1 d \cosh k_2 d}\right\} \cos \omega^- t - a_1 a_2 2\omega^- g^{-1} Y \cosh K^- d \sin \omega^- t,\end{aligned} \tag{30}$$

where X and Y are defined in the appendix. If this equation is written in the form

$$\tilde{\eta}^{(2)} = \bar{\zeta}\cos(\omega^{-}t+\beta)$$

the values of $\bar{\zeta}$ appropriate to the experiments already described can be calculated. These values are shown as the theoretical curves joining squares in figures 4(*a*)–(*c*). They have been plotted as positive quantities since the coefficient of $\cos\omega^{-}t$ in (30) is now positive, implying that when the two primary waves are in phase ($\omega^{-}t = 2n\pi$) a set-up should occur.

It is clear that better agreement is obtained between theory and experiment when the secondary wave introduced by the wave paddle is included. These results can be taken as verifying the existence of secondary waves when groups are generated in model experiments. Bowers (1976) has given indirect evidence for their existence in a comparison between theory and model experiments on the long-period oscillations of a moored ship caused by wave grouping. Good agreement was obtained only when secondary waves at the group periods were taken into account.

The secondary wave generated by the paddle in the case where the difference between the frequencies of the two primary waves equalled the frequency of the sloshing mode also happened to be close to a resonant mode of the wave flume of length L outside the resonator, i.e. $\sin K^{-}L \simeq 0$. For this reason the theoretical value of the secondary wave amplitude was much larger than the set-down amplitude. This explains the large values corresponding to the squares in figure 4(*c*). As mentioned in the appendix, the experimental response of the wave flume to monofrequency waves was found to display only small resonant peaks at low frequencies. This was probably due to losses between the flume walls and the paddle face. For this reason the secondary wave was unlikely to be amplified to the extent predicted by theory and this could explain why, in figure 4(*c*), the set-up observed was smaller than that predicted.

Having accepted the existence of a secondary wave with the group period it is clear that it will excite a large response in the resonator when the group period is close to a resonant period. However, the theory presented in the last section indicates that the resonator should also respond to the set-down associated with the wave groups. In particular, since the primary wave heights inside the resonator are smaller than those outside, the resonator should respond to the set-down outside as if it were a real long wave. Thus one would expect the resultant of the secondary wave and the set-down to be amplified. In order to test this theory figures 7(*a*)–(*c*) have been plotted.

Figure 7(*a*) shows the wave amplitude along the back wall of the resonator plotted against the square root of the product of the two primary wave amplitudes for the case $f_1 = 1{\cdot}0$ Hz with $f_2 - f_1 = 0{\cdot}0475$ Hz (the Helmholtz frequency). The experimental values measured by the wave recorder are indicated by crosses. The curve joining triangles was obtained by calculating the amplitude of the secondary wave outside the resonator from the formula

$$\eta = \phi_t^{(2)}/g, \tag{31}$$

where $\phi_t^{(2)}$ is given by equation (A 4) in the appendix, reading off the amplification factor corresponding to that amplitude for the Helmholtz resonance from

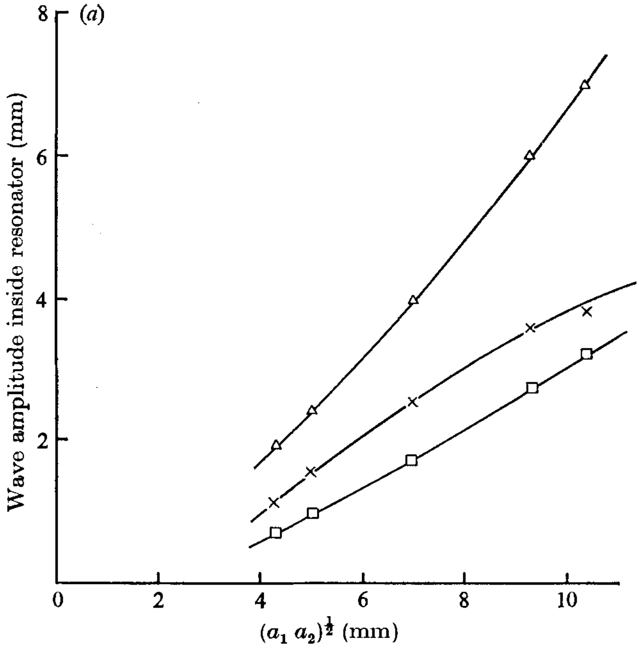

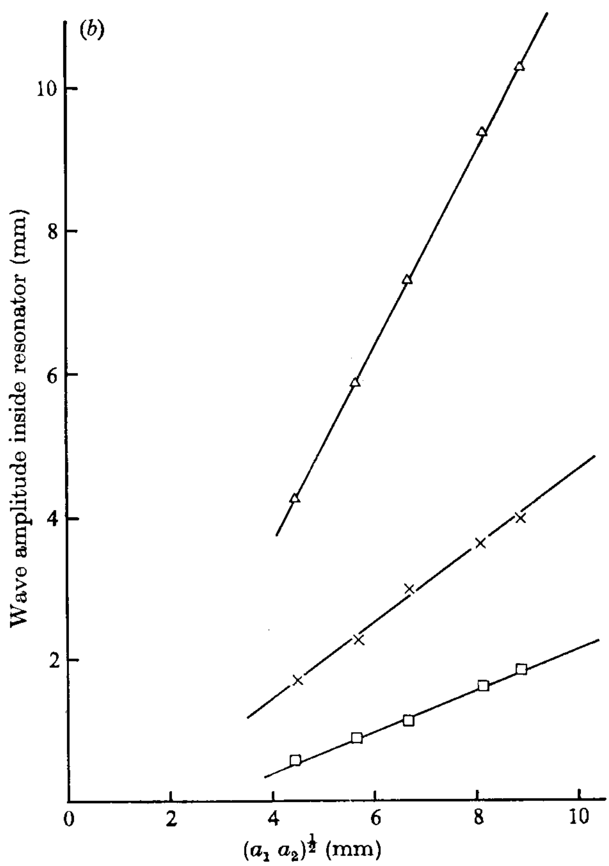

FIGURES 7 (*a*, *b*). For caption see p. 90.

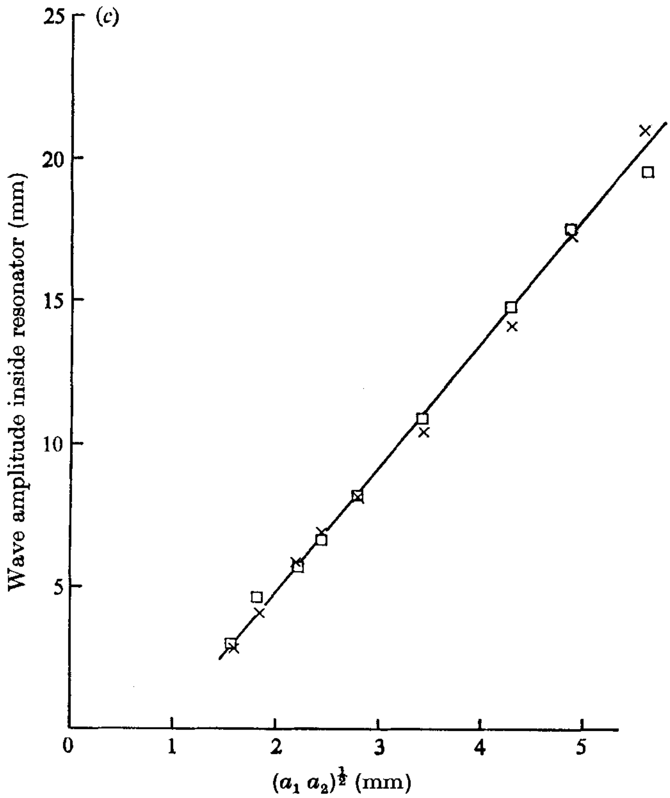

FIGURE 7. Amplitude of the resonant wave *vs.* $(a_1 a_2)^{\frac{1}{2}}$ for (*a*) $f_1 = 1{\cdot}0$ Hz, $f_2 = 1{\cdot}0475$ Hz, (*b*) $f_1 = 0{\cdot}6$ Hz, $f_2 = 0{\cdot}6475$ Hz and (*c*) $f_1 = 0{\cdot}65$ Hz, $f_2 = 0{\cdot}99$ Hz. ×, experimental values. (*a*), (*b*) □, theoretical values obtained assuming resultant of set-down and secondary wave is amplified; △, theoretical values obtained assuming only secondary wave is amplified. (*c*) □, theoretical values obtained assuming only measured set-up is amplified.

figure 3(*a*) and multiplying together the amplification factor and the amplitude. If the resonator were responding only to the secondary wave this curve should agree with the experimental curve through crosses. The curve through the squares was obtained by calculating the amplitude of the resultant of the secondary wave and the set-down outside the resonator from (31), where $\phi^{(2)}$ is now the sum of the potentials given in (A 4) and (27), reading off the amplification factor corresponding to that amplitude from figure 3(*a*) and multiplying together the amplification factor and the amplitude. If the resonator were responding to the resultant of the secondary wave and the set-down this curve should agree with the experimental curve.

Figure 7(*b*) is a similar plot to figure 7(*a*) but with $f_1 = 0{\cdot}6$ Hz and $f_2 - f_1 = 0{\cdot}0475$ Hz. Figure 7(*c*) is a plot of the wave amplitude at the antinode in the entrance channel of the resonator against the same function of primary wave amplitude for $f_1 = 0{\cdot}65$ Hz with $f_2 - f_1 = 0{\cdot}34$ Hz (the frequency of the sloshing mode). The difference here is that only a theoretical curve through squares is plotted, together with the curve giving the experimental wave heights measured inside the resonator. The curve through the squares was obtained by reading off from figure 4(*c*) the set-up measured outside the resonator and multiplying this value by the appropriate amplification factor for the sloshing mode given in figure 3(*b*). The experimental value of the set-up was used here instead of a calculated value because the calculated value was too large for the reason given when discussing figure 4(*c*). Since the measured set-up will be the resultant of the secondary wave and the set-down, squares are used to label the theoretical curve in figure 7(*c*).

Taking figures 7(*a*)–(*c*) together, the results indicate that the resonator responded to the resultant of the set-down and the secondary free wave rather than to just the secondary wave. This implies that in a real sea one can expect harbour resonances to be excited by set-down beneath wave groups.

One important point brought out in the experimental work is that, although set-down increases as the square of the primary wave height, the height of resonant long waves excited inside the harbour by set-down will be more nearly proportional to the primary wave height itself. This is demonstrated by the plots in figure 7, where straight lines were obtained instead of a square-law increase with primary wave amplitude. The reason is simply that, as the primary wave height increases, the square-law increase in the amplitude of the resonant wave excited by set-down is counteracted by the decrease in the amplification factor owing to flow separation in the harbour entrance.

I am grateful to Mr G. Lean and Mr G. Gilbert for many helpful discussions. The work described here is part of the research programme at the Hydraulics Research Station, Wallingford, and the paper is published by permission of the Director of Hydraulics Research.

Appendix. Calculation of the velocity potential of the secondary wave

The potential of the secondary wave is determined by the boundary condition on the face of the wave paddle. Since the paddle was programmed to produce only two sine waves of slightly different frequency there was no second-order paddle movement. Therefore, the boundary condition on the paddle face is

$$u_x^{(2)} = 0.$$

Denoting the paddle movement by $\xi^{(1)}$, this condition can be expressed in the form

$$\phi_x^{(2)} + \xi^{(1)}\phi_{xx}^{(1)} = 0, \tag{A 1}$$

where $\phi^{(2)}$ is the sum of the potentials due to the set-down and the secondary wave and the whole expression is evaluated at the mean position of the paddle, $x = L$.

The first-order paddle movement is related to the primary wave amplitudes by a transfer function. This function will be dependent on reflexions from the paddle of waves that have already reflected once from the wall at the end of the flume ($x = 0$). Looking at the experimental set-up shown in figure 2 one might expect quite small paddle movements at a resonant period of the flume to lead to large wave amplitudes. In order to test whether such resonances were present the response of the wave flume to monofrequency waves was examined. It was found that small resonant peaks were obtained at low frequencies but that, although predicted theoretically, no resonances were apparent in the range of frequencies covering the primary wave systems used in the experimental work. This could have been due to losses through the gap between the paddle face and the ends of the flume walls. This gap had to be present to allow for movement of the paddle back and forth. For this reason the usual transfer function relating the paddle movement to the amplitude of a progressive wave propagating away from the paddle is assumed. Thus, for a primary wave system consisting of two frequencies,

$$\xi^{(1)} = -\sum_{j=1,2} \frac{a_j n_j}{\tanh k_j d} \sin(\omega_j t + k_j L), \tag{A 2}$$

where

$$n_j = \tfrac{1}{2}(1 + 2k_j d/\sinh 2k_j d).$$

Denoting the potential of the secondary wave by $\phi^{(2)}_{sw}$ and the second-order Stokes potential by $\phi^{(2)}_s$, equation (A 1) can be put in the form

$$\phi^{(2)}_{swx} = -\phi^{(2)}_{sx} - \xi^{(1)}\phi^{(1)}_{xx}. \tag{A 3}$$

Then the potential of the secondary wave fluctuating at the group frequency is determined by evaluating the slowly varying part of the right-hand side of (A 3) using (27) for $\phi^{(2)}_s$, (28) for $\phi^{(1)}$ and (A 2) for $\xi^{(1)}$. This potential $\phi^{(2)}_{sw}$, which must also satisfy the usual boundary conditions on a surface wave, is found to be

$$\begin{aligned}\phi^{(2)}_{sw} = a_1 a_2 \cosh K^-(z+d)\,[&X\{\sin(\omega^- t + K^- x) + \sin(\omega^- t - K^- x)\} \\ &+ Y\{\cos(\omega^- t + K^- x) + \cos(\omega^- t - K^- x)\}],\end{aligned} \tag{A 4}$$

where

$$X = -\frac{Ak^- \sin k^- L}{K^- \sin K^- L} - \frac{g}{2dK^- \sin K^- L}\left(\frac{k_1 n_2 \tanh k_1 d}{\omega_1 \tanh k_2 d}\sin k_2 L \cos k_1 L - \frac{k_2 n_1 \tanh k_2 d}{\omega_2 \tanh k_1 d}\sin k_1 L \cos k_2 L\right),$$

$$Y = -\frac{g \cos k_1 L \cos k_2 L}{2dK^- \sin K^- L}\left(\frac{k_1 n_2 \tanh k_1 d}{\omega_1 \tanh k_2 d} + \frac{k_2 n_1 \tanh k_2 d}{\omega_2 \tanh k_1 d}\right).$$

REFERENCES

Bowen, A. J. & Inman, D. L. 1971 *J. Geophys. Res.* **76**, 8662.

Bowers, E. C. 1976 *Trans. Roy. Inst. Naval Archit.* **118**, 181.

Clarke, D. J. 1974 *Dock Harbour Authority*, **54**, 383.

Longuet-Higgins, M. S. & Stewart, R. W. 1964 *Deep-Sea Res.* **11**, 529.

Saville, T. 1961 *Proc. 2nd Tech. Conf. Hurricanes, Miami Beach, Fla*, p. 242. *Nat. Hurricane Res. Proj. Rep.* no. 50.

Tucker, M. J. 1950 *Proc. Roy. Soc.* A **207**, 565.

Wilson, B. W. 1957 *Permanent Int. Ass. Navig. Cong. London*, §2, comm. 1.